J. Phys. B: At. Mol. Phys. **20** (1987) 1823-1838. Printed in the UK

Electron impact multiple ionisation of multiply charged krypton ions†

K Tinschert‡, A Müller‡, R Becker§ and E Salzborn‡

‡ Institut für Kernphysik, Universität Giessen, D-6300 Giessen, West Germany
§ Institut für Angewandte Physik, Universität Frankfurt, D-6000 Frankfurt, West Germany

Received 26 August 1986

Abstract. Absolute cross sections for double ionisation of Kr^{q+} ions ($q = 1, \ldots, 4$) and for triple ionisation of Kr^{q+} ions ($q = 1, 2$) in single collisions with incident electrons have been measured by using a dynamic crossed-beams technique. Electron energies ranged from below threshold up to 1000 eV for Kr^{2+} and up to 700 eV for the other charge states. With increasing q the cross sections for double ionisation are determined by an increasing relative contribution of single ionisation of the 3d subshell and subsequent autoionisation. Our data for double ionisation of Kr^{4+} are in good agreement with measurements of Pindzola *et al.* For electron energies above 300 eV triple ionisation appears to be dominated by ionisation-double-autoionisation contributions from the 3p and 3s subshells. Between threshold and about 200 eV, however, the observed cross sections $\sigma_{q,q+3}$ seem to be due to direct multiple-electron processes.

1. Introduction

Electron impact multiple ionisation of ions was first studied by Peart and Dolder (1969). They measured cross sections $\sigma_{1,3}$ for double ionisation of Li^+ ions and found the maximum to be below 10^{-20} cm^2. For multiply charged ions it was not before 1980 that the first direct measurements of multiple ionisation were reported (Müller and Frodl 1980). This work on Ar^{q+} ions ($q = 1, 2, 3$) clearly demonstrated the importance of inner-shell ionisation with subsequent autoionisation. In addition, the measurements suggested that this indirect mechanism becomes progressively more dominant over direct multiple ionisation for the more highly charged Ar ions. Recent investigations of double ionisation of Ar^{4+} ions confirmed this trend and for Ar^+ ions the indirect contribution of the L shell could be clearly identified (Müller *et al* 1985b, Pindzola *et al* 1984). Multiple ionisation of Xe^{q+} ions also shows increasing relative contributions from 4d subshell ionisation-autoionisation as q changes from one to four (Müller *et al* 1984, Pindzola *et al* 1984). Recently, however, Howald *et al* (1986) reported high contributions of multiple-target-electron processes to triple ionisation of Xe^{6+} ions, an observation that was unexpected considering the previous multiple ionisation studies along the Xe isonuclear sequence.

Double ionisation cross sections for Xe^+ and I^+ (and less pronounced also for Xe^{2+}, Xe^{3+} and Xe^{4+} ions) showed a dominant resonance-like feature which, both in shape and size, almost coincides with the partial 4d-photoionisation cross section of Xe atoms (Achenbach *et al* 1983). Pindzola *et al* (1983, 1984) tried to explain this

† Work supported by Deutsche Forschungsgemeinschaft.

feature by term dependence in the continuum for the 4d ionisation mechanism. Another concept was proposed by Younger (1986) who found evidence for giant resonances in the electron impact ionisation of heavy atoms and ions.

Recent studies of $Sb^{q+}(q=1,2)$ and $Bi^{q+}(q=1,2,3)$ ions revealed the effects of collision-strength shifts between single and double ionisation depending on the initial ion charge state. Furthermore, extremely large cross sections with maxima up to 8×10^{-17} cm^2 were found for double ionisation of these ions (Müller *et al* 1985d).

The high multiple ionisation probabilities for complex ions can lead to important influences on the charge-state evolution of ions in hot plasmas (Müller 1986).

Theory on electron impact multiple ionisation of atoms and ions has not been developed beyond the classical binary encounter approximation for the ejection of two electrons (BEA2) of Gryzinski (1965) and the applicability of this calculation is doubtful. In this paper we try to separate multiple from direct single ionisation of inner shell electrons with subsequent autoionisation. Cross sections for these processes can be well estimated by using the BEA1 theory for ionisation of a single electron (Gryzinski 1965). Our investigation reveals an increasing relative contribution of 3d ionisation–autoionisation to $\sigma_{q,q+2}$ for Kr^{q+} ions as the ion charge state q increases.

The cross sections $\sigma_{4,6}$ for Kr^{4+} ions, which are in good agreement with data of the Oak Ridge group (Pindzola *et al* 1984), appear to be completely dominated by the indirect process via the 3d subshell. The main contributions to triple ionisation of Kr^{+} and Kr^{2+} ions are from the inner shells 3p and 3s.

2. Experimental technique

The crossed-beams arrangement and experimental techniques employed to measure ionisation cross sections have already been described in detail (Müller *et al* 1985a, Tinschert *et al* 1987). In brief, beams of multiply charged krypton ions are extracted from an electron-beam ion source and accelerated by a voltage of 10 kV. A 90° analysing magnet selects ions of a given mass and charge. The ion beam is collimated to a diameter of between 0.2 and 0.7 mm before it is passed through the high-current electron beam. During a cross section measurement, the electron gun is moved perpendicularly up and down across the ion beam with constant velocity, sweeping over a range from complete separation over complete overlap onto complete separation of the two beams. The ionised product ions are separated from the parent ion beam by a second analysing magnet. The count rate of product ions, the parent ion current I_i and the actual velocity of the electron gun movement are registered simultaneously by a multichannel analyser as a function of the electron gun displacement. Without any further measurements of beam overlap factors, it is possible to evaluate absolute cross sections by using the relation (Müller *et al* 1985c)

$$\sigma=\frac{S\,\Delta z}{MI_e\varepsilon}. \tag{1}$$

The content of each channel of the signal spectrum corresponding to an electron gun displacement Δz and an integration time of about $\Delta t=0.1$ s is divided by the content of the corresponding channel of the parent ion current spectrum containing the accumulated ion charge. Thus a normalised signal spectrum is generated. S is the peak area in this normalised spectrum resulting from the overlap of the two beams

and I_e is the total electron current. The factor M is given by

$$M = (v_e^2 + v_i^2)^{1/2}/(v_e v_i q e^2) \tag{2}$$

where $v_e(v_i)$ is the electron (ion) velocity in the electron (ion) beam. The efficiency of the ion detector is $\varepsilon = 0.97 \pm 0.03$. The following systematic experimental uncertainties have to be taken into account: uncertainties of beam currents I_i and $I_e(\pm 3\%)$, particle velocities v_i and v_e $(\pm 1\%)$, detector efficiency $(\pm 3\%)$ and the electron gun displacement $\Delta z(\pm 0.6\%)$. The probable *total* error is given by the quadrature sum of the statistical counting error at the 95% confidence level and the individual systematic uncertainties estimated at a comparable level of confidence.

3. Results and discussion

3.1. Double ionisation

Electron impact double ionisation cross sections $\sigma_{q,q+2}$ for the processes

$$e + Kr^{q+} \rightarrow Kr^{(q+2)+} - 3e \qquad q = 1, \ldots, 4 \tag{3}$$

were measured in the electron energy range from below threshold up to 700 eV (1000 eV for Kr^{2+} ions). The data are listed in table 1 together with their total uncertainty at the 95% confidence level for the statistical error. The measured cross sections $\sigma_{q,q+2}(q = 1, \ldots, 4)$ are displayed in figure 1. The error bars shown in figure 1 indicate the statistical uncertainties only. The broken curves are direct single ionisation cross sections for the 3d subshell calculated from the binary encounter approximation (BEA1 (Gryzinski 1965)) for single ionisation from one subshell:

$$\sigma_{q,q+2}^{\mathrm{BEA1}} = \sigma_0 g(x) n / P^2. \tag{4}$$

They indicate the possible contribution to $\sigma_{q,q+2}$ from 3d ionisationautoionisation processes.

In equation (4) $\sigma_0 = 6.56 \times 10^{-14}\,\mathrm{cm^2\,eV^2}$, $x = E/P$, E is the electron energy, P is the ionisation potential and n is the number of electrons in the subshell. The shape of the cross section is determined by a function $g(x)$ which is given in analytical form by Gryzinski (1965). The BEA1 results are usually close to the predictions of the Lotz formula (Lotz 1968). The ionisation potentials of the 3d subshell in Kr^{q+} ions are 105 $(q = 1)$, 120 $(q = 2)$, 135 $(q = 3)$ and 152 eV $(q = 4)$. However, the threshold energies of the measured cross sections coincide with the minimum energies required for direct double ionisation, i.e. 61.3 $(q = 1)$, 87 $(q = 2)$, 113 $(q = 3)$ and 141 eV $(q = 4)$. Thus the measurements indicate contributions to the cross sections other than ionisation-autoionisation processes.

The measured cross sections $\sigma_{2,4}$, $\sigma_{3,5}$ and $\sigma_{4,6}$ show a similar rise from their respective thresholds to their maxima, which are at about 500 eV electron energy. In contrast, $\sigma_{1,3}$ increases much more steeply, reaches a maximum at about 150 eV and there is an indication of a change in slope at about 300 eV. A further comparison can be made with the cross section $\sigma_{0,2}$ for the electron impact ionisation of neutral Kr atoms, where measurements of Stephan *et al* (1980) in the low-energy range between threshold and 180 eV and of Nagy *et al* (1980) for electron energies above 500 eV are available. Regrettably, no experimental data exist for the interesting energy range between 180 and 500 eV where changes in the cross section course could be expected. Similar to $\sigma_{1,3}$, the cross section $\sigma_{0,2}$ shows a very steep rise directly above the threshold

Table 1. Electron impact double ionisation cross sections $\sigma_{q,q+2}(q = 1, 2, 3, 4)$ for Kr^{q+} ions. Estimated total uncertainties are given including the statistical error at the 95% confidence level.

Electron energy (eV)	Cross section (10^{-18} cm^2)	Electron energy (eV)	Cross section (10^{-18} cm^2)
$\sigma_{1,3}$: $Kr^+ \rightarrow Kr^{3+}$			
50.0	0.00 ± 0.02	240.0	10.5 ± 0.7
52.6	0.00 ± 0.04	243.0	10.5 ± 0.7
57.6	0.04 ± 0.05	250.0	10.4 ± 0.6
60.0	0.05 ± 0.02	260.0	10.2 ± 0.6
60.5	0.07 ± 0.02	265.0	10.4 ± 0.6
62.6	0.25 ± 0.03	281.0	10.4 ± 0.6
64.9	0.82 ± 0.06	285.0	10.2 ± 0.6
67.5	1.43 ± 0.10	295.0	10.0 ± 0.6
70.5	2.49 ± 0.16	300.0	9.65 ± 0.60
71.1	3.20 ± 0.25	310.0	10.2 ± 0.6
75.2	5.00 ± 0.40	320.0	9.76 ± 0.61
80.0	6.07 ± 0.38	330.0	10.3 ± 0.6
81.2	6.41 ± 0.43	340.0	9.73 ± 0.60
85.1	7.36 ± 0.49	350.0	10.1 ± 0.6
92.3	8.77 ± 0.58	360.0	9.66 ± 0.59
94.7	8.68 ± 0.56	370.0	9.87 ± 0.61
100.0	9.68 ± 0.60	380.0	9.59 ± 0.59
102.0	9.49 ± 0.61	389.0	10.1 ± 0.6
110.0	10.3 ± 0.7	400.0	9.61 ± 0.60
120.0	11.2 ± 0.7	415.0	9.88 ± 0.61
128.0	11.6 ± 0.7	425.0	9.57 ± 0.60
135.0	11.6 ± 0.7	440.0	9.77 ± 0.61
143.0	11.9 ± 0.7	450.0	9.52 ± 0.59
150.0	11.9 ± 0.7	465.0	9.65 ± 0.60
157.0	11.6 ± 0.7	475.0	9.41 ± 0.59
164.0	11.8 ± 0.7	490.0	9.47 ± 0.59
172.0	11.7 ± 0.7	500.0	9.46 ● 0.59
180.0	11.3 ± 0.7	515.0	9.36 ± 0.58
185.0	11.6 ± 0.7	525.0	8.86 ± 0.55
193.0	11.4 ± 0.7	540.0	9.11 ± 0.56
200.0	10.7 ± 0.7	550.0	9.48 ± 0.59
201.0	11.3 ± 0.7	570.0	8.92 ± 0.55
205.0	10.8 ± 0.7	600.0	8.90 ± 0.55
215.0	11.2 ± 0.7	650.0	8.69 ± 0.54
228.0	11.1 ± 0.7		
$\sigma_{2,4}$: $Kr^{2+} \rightarrow Kr^{4+}$			
50.0	0.01 ± 0.10	150.0	4.16 ± 0.26
60.0	0.10 ± 0.19	170.0	4.79 ± 0.33
70.0	−0.23 ± 0.08	200.0	5.38 ± 0.35
75.0	0.09 ± 0.14	220.0	5.93 ± 0.37
80.0	−0.02 ± 0.04	250.0	6.22 ± 0.39
85.0	0.03 ± 0.05	300.0	6.49 ± 0.41
88.0	0.14 ± 0.05	350.0	6.90 ± 0.43
90.0	0.26 ± 0.06	400.0	6.97 ± 0.43
95.0	0.67 ± 0.09	450.0	7.10 ± 0.44
100.0	1.03 ± 0.09	500.0	7.05 ± 0.44
105.0	1.56 ± 0.12	600.0	7.02 ± 0.44
110.0	1.92 ± 0.13	700.0	6.94 ± 0.43
120.0	2.63 ± 0.18	850.0	6.67 ± 0.41
135.0	3.55 ± 0.24	1000.0	6.30 ± 0.38

Table 1. (continued)

Electron energy (eV)	Cross section (10^{-18} cm^2)	Electron energy (eV)	Cross section (10^{-18} cm^2)
$\sigma_{3,5}$: $Kr^{3+} \rightarrow Kr^{5+}$			
70.0	-0.38 ± 0.84	250.0	4.96 ± 0.52
80.3	-0.25 ± 0.67	260.0	5.15 ± 0.51
89.7	0.03 ± 0.63	270.0	5.32 ± 0.51
100.0	0.14 ± 0.49	280.0	5.56 ± 0.51
105.0	0.13 ± 0.16	290.0	5.65 ± 0.49
110.0	0.12 ± 0.22	300.0	5.76 ± 0.48
115.0	0.03 ± 0.32	310.0	5.97 ± 0.49
121.0	0.44 ± 0.20	320.0	6.04 ± 0.49
130.0	0.80 ± 0.22	330.0	6.09 ± 0.49
133.0	1.13 ± 0.24	340.0	6.20 ± 0.50
140.0	1.20 ± 0.25	350.0	6.29 ± 0.50
142.0	1.55 ± 0.27	375.0	6.20 ± 0.48
145.0	1.62 ± 0.26	380.0	6.53 ± 0.50
146.0	2.01 ± 0.37	400.0	6.54 ± 0.50
150.0	2.11 ± 0.35	410.0	6.80 ± 0.51
152.0	1.92 ± 0.30	421.0	6.58 ± 0.49
160.0	2.26 ± 0.37	431.0	6.90 ± 0.52
165.0	2.47 ± 0.37	461.0	6.86 ± 0.51
170.0	2.64 ± 0.39	481.0	6.97 ± 0.51
175.0	2.90 ± 0.40	500.0	6.71 ± 0.48
180.0	3.18 ± 0.44	515.0	6.71 ± 0.48
190.0	3.27 ± 0.44	540.0	7.18 ± 0.51
200.0	3.74 ± 0.48	570.0	7.02 ± 0.50
210.0	4.03 ± 0.49	599.0	6.73 ± 0.48
220.0	4.31 ± 0.51	635.0	6.84 ± 0.49
230.0	4.49 ± 0.51	670.0	6.54 ± 0.47
240.0	4.85 ± 0.44	700.0	6.67 ± 0.48
$\sigma_{4,6}$: $Kr^{4+} \rightarrow Kr^{6+}$			
100.0	0.32 ± 0.39	340.0	5.31 ± 0.39
110.0	0.17 ± 0.46	360.0	5.54 ± 0.39
120.0	0.39 ± 0.64	380.0	5.84 ± 0.41
130.0	-0.19 ± 0.31	400.0	5.85 ± 0.40
140.0	-0.08 ± 0.28	420.0	6.09 ± 0.41
145.0	0.36 ± 0.28	440.0	6.07 ± 0.40
150.0	0.45 ± 0.25	461.0	6.07 ± 0.41
160.0	0.58 ± 0.22	470.0	6.34 ± 0.45
170.0	0.89 ± 0.31	480.0	6.22 ± 0.42
181.0	1.49 ± 0.42	500.0	6.22 ± 0.42
191.0	1.82 ± 0.30	510.0	6.54 ± 0.42
200.0	2.06 ± 0.32	525.0	6.33 ± 0.42
210.0	2.42 ± 0.32	550.0	6.45 ± 0.43
215.0	2.78 ± 0.21	575.0	6.53 ± 0.43
220.0	2.77 ± 0.29	580.0	6.58 ± 0.42
225.0	3.27 ± 0.26	590.0	6.48 ± 0.41
240.0	3.44 ± 0.31	600.0	6.57 ± 0.42
250.0	3.89 ± 0.35	620.0	6.42 ± 0.41
260.0	3.86 ± 0.33	640.0	6.39 ± 0.41
270.0	4.37 ± 0.29	660.0	6.23 ± 0.40
280.0	4.46 ± 0.38	680.0	6.58 ± 0.42
300.0	4.76 ± 0.38	700.0	6.59 ± 0.42
320.0	5.02 ± 0.38		

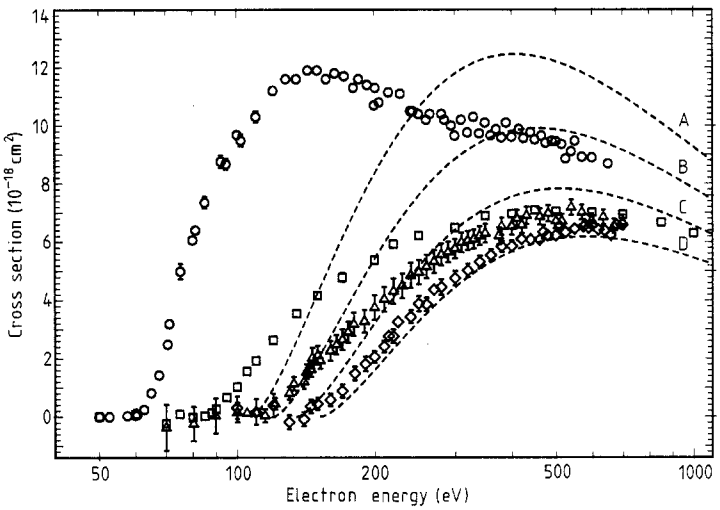

Figure 1. Present measurements of cross sections $\sigma_{q,q+2}(q = 1, \ldots, 4)$ for double ionisation of Kr^{q+}: ○, $\sigma_{1,3}$; □, $\sigma_{2,4}$; Δ, $\sigma_{3,5}$; ◇, $\sigma_{4,6}$. Error bars show the statistical error at the 95% confidence level. The broken curves represent the results of the semiclassical binary encounter approximation (BEA1, Gryzinski 1965) for single ionisation of a 3d electron: curve A, $\sigma_{1,3}^{BEA1}(3d)$; curve B, $\sigma_{2,4}^{BEA1}(3d)$; curve C, $\sigma_{3,5}^{BEA1}(3d)$; curve D, $\sigma_{4,6}^{BEA1}(3d)$.

and reaches a maximum of 3×10^{-17} cm^2 at about 100 eV. Beyond the maximum the cross section falls off rapidly, reaching the same absolute value as the cross sections $\sigma_{q,q+2}(q = 1, \ldots, 4)$ for energies above 700 eV. This behaviour is similar to that observed for $\sigma_{1,3}$. So the comparison in figure 1 and the consideration of $\sigma_{0,2}$ suggest a dominating influence of 3d inner-shell ionisation-autoionisation for Kr^{2+}, Kr^{3+} and Kr^{4+} ions and a strong additional mechanism of double ionisation for Kr^+ ions, as well as for neutral Kr atoms.

In the following the results for each ion will be discussed in more detail separately.

3.1.1. Kr^+ double ionisation. Figure 2 shows the measured double ionisation cross sections for Kr^+ ions together with the total uncertainties. The broken curve is 0.8 $\sigma_{1,3}^{BEA1}$ (see equation (4)) representing a 3d-ionisation-autoionisation contribution to $\sigma_{1,3}$, which might explain the experimental data at energies above 300 eV but obviously cannot account for the results observed below 105 eV. Since $\sigma_{1,3}$ increases immediately above the threshold for direct ejection of two electrons from the 4p subshell, one might conclude that the low-energy part of $\sigma_{1,3}$ is due to the direct double-electron process. The only theoretical approach to this process is the classical BEA2 theory of Gryzinski (1965) which predicts

$$\sigma_{q,q+2}^{BEA2} = \frac{\sigma_0^2}{P_1^2 P_2^2} \frac{n_e^{5/3}(n_e - 1)}{4\pi R^2} g_{ii}\left(\frac{E}{P_1 + P_2}\right). \tag{5}$$

for the cross section. Here, σ_0 is the same as in equation (4), P_1 and P_2 are the ionisation potentials of the ions Kr^{q+} and $Kr^{(q+1)+}$, n_e is the number of electrons in the outermost shell of the parent ion, R is the gas-kinetic radius of the ion and the general function g_{ii} is as in Gryzinski's paper. The values for R were taken from Fraga *et al* (1976).

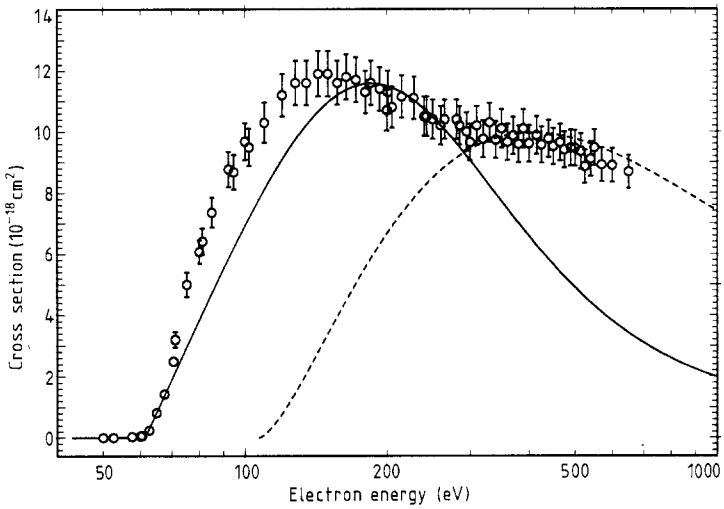

Figure 2. Comparison of the measured cross sections $\sigma_{1,3}$ for double ionisation of Kr^+ (error bars show the total experimental uncertainties) with the prediction of the binary encounter approximation (BEA, Gryzinski 1965) for direct double ionisation of Kr^+ ions ($\sigma_{1,3}^{BEA2}$) scaled by a factor of 0.2 (full curve). Also shown is $\sigma_{1,3}^{BEA1}(3d)$ (see figure 1) scaled by a factor of 0.8 (broken curve, with onset at the 3d-ionisation threshold).

The full curve in figure 2 represents $0.2\sigma_{1,3}^{BEA2}$. As has already been shown for Ar^+ (Müller *et al* 1985b), the BEA2 theory can greatly overestimate the size but may reproduce the shape of a double ionisation cross section reasonably well. With this empirical result in mind, the full curve appears to be in acceptable agreement with the measurements at low electron energies. However, a simple addition of weighted contributions $a\sigma_{1,3}^{BEA2}$ and $b\sigma_{1,3}^{BEA1}$ does not fit the data, regardless of which combination of a and b is chosen. It would also be difficult to accept a supposition of interference of the individual contributions such that the measured cross sections result. Hence the assumption of two contributions from direct double ionisation and 3d-ionisation-autoionisation may be inadequate. We suggest, rather, looking at a mechanism similar to the one that produced a resonance-like cross section contribution to $\sigma_{1,3}$ for Xe^+ and I^+ ions (Achenbach *et al* 1983). This mechanism would involve the 3d subshell, either with ionisation-autoionisation or with excitation-double-autoionisation processes (such as $3d^94s^24p^6 \rightarrow 3d^{10}4s^24p^3$). Pindzola *et al* (1984) have theoretically produced similar cross section shapes by considering term dependence and ground-state correlations in their calculations. Recently, Younger (1986) has described the calculation of shape resonances which occur in the scattering channel and lead to cross section curves (e.g. for the electron impact double ionisation of Cs^+ ions) which are similar in shape to the present cross section $\sigma_{1,3}$. Obviously, this phenomenon observed in ionisation cross sections is going to become a testing ground for theoretical descriptions of complex atoms and ions and their collision processes.

3.1.2. Kr^{2+} double ionisation. Figure 3 shows the measured double ionisation cross sections for Kr^{2+} ions together with the total uncertainties. The broken curve is $0.70\sigma_{2,4}^{BEA1}$ (see equation (4)), representing a 3d-ionisation-autoionisation contribution to $\sigma_{2,4}$ which fits the experimental data at energies above 200 eV. The full curve is $0.75\sigma_{2,4}^{BEA2}$ (see equation (5)) and thus represents a contribution from direct double

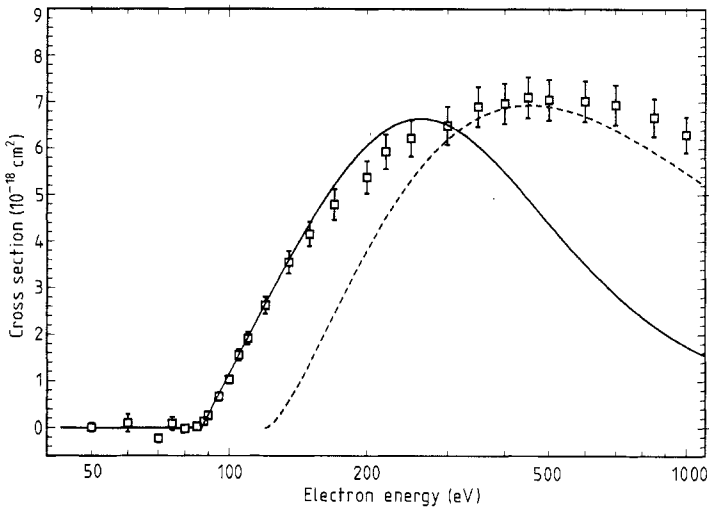

Figure 3. Comparison of the measured cross sections $\sigma_{2,4}$ for double ionisation of Kr^{2+} (error bars show the total experimental uncertainties) with the prediction of the BEA for direct double ionisation ($\sigma_{2,4}^{BEA2}$) scaled by a factor of 0.75 (full curve). Also shown is $\sigma_{2,4}^{BEA1}(3d)$ (see figure 1) scaled by a factor of 0.7 (broken curve, with onset at the 3d-ionisation threshold)

ionisation of two electrons from the $n=4$ shell. It is in good agreement with the experimental data at energies below the 3d-ionisation threshold.

As in the case of Kr^+ ions, any simple addition of weighted contributions $a\sigma_{2,4}^{BEA2}$ and $b\sigma_{2,4}^{BEA1}$ would not fit the data. Again, it would be difficult to accept the assumption of an interference between the two contributions just leading to the observed cross section.

In contrast to the Kr^+ case, the cross section $\sigma_{2,4}$ does not show the steep increase at energies above the double ionisation threshold.

3.1.3. Kr^{3+} double ionisation. Figure 4 shows the measured double ionisation cross sections for Kr^{3+} ions together with the total uncertainties. The broken curve is $0.85\sigma_{3,5}^{BEA1}$ (see equation (4)), representing a 3d-ionisation–autoionisation contribution to $\sigma_{3,5}$ which fits the experimental data at energies above 300 eV. The full curve is the BEA2 result from equation (5) and and represents the contribution from direct double ionisation of two electrons from the $n=4$ shell. While for Kr^+ and Kr^{2+} ions the BEA2 cross sections had to be scaled by factors of less than one to obtain agreement with some of the experimental data, the BEA2 result is now a factor of two below the cross sections measured at energies between the threshold for the direct double ionisation process and the 3d single ionisation (which is then followed by autoionisation).

A simple addition of the two contributions may give a reasonable overall representation of the experimental data for Kr^{3+}, but the structure which is then to be expected at the threshold of 3d ionisation does not show up in the measurements.

3.1.4. Kr^{4+} double ionisation. Figure 5 shows the measured double ionisation cross sections for Kr^{4+} ions together with the total uncertainties. The figure includes the

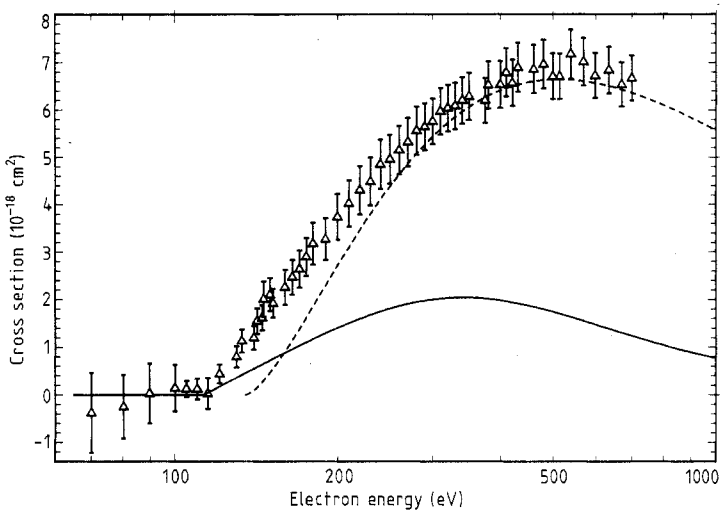

Figure 4. Comparison of the measured cross sections $\sigma_{3,5}$ for double ionisation of Kr^{3+} (error bars show the total experimental uncertainties) with the prediction of the BEA for direct double ionisation ($\sigma_{3,5}^{BEA2}$, full curve). Also shown is $\sigma_{3,5}^{BEA1}(3d)$ (see figure 1) scaled by a factor of 0.85 (broken curve, with onset at the 3d-ionisation threshold).

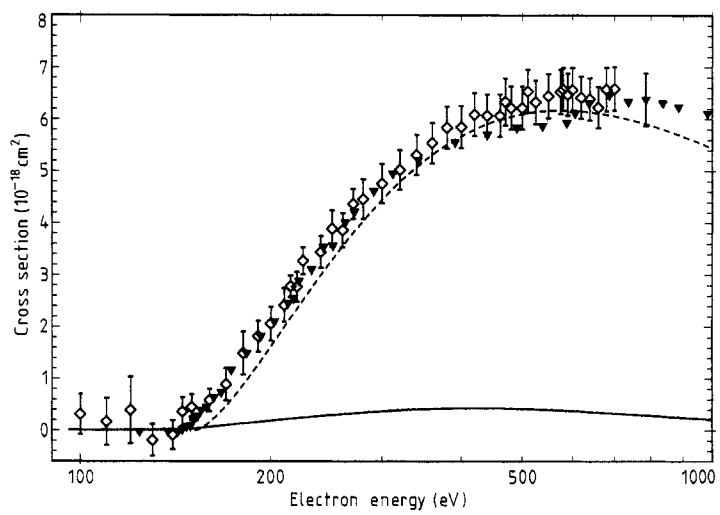

Figure 5. Cross sections $\sigma_{4,6}$ for the double ionisation of Kr^{4+} ions. ◇, present measurements; error bars show total experimental uncertainties. ▼, measurements of the Oak Ridge group (Pindzola *et al* 1984); total experimental uncertainty is quoted to be ±8% at the peak of the cross section (see representative error bar at 785 eV). The full curve represents the prediction of the BEA for direct double ionisation $\sigma_{4,6}^{BEA2}$ and the broken curve (onset at the 3d-ionisation threshold) shows $\sigma_{4,6}^{BEA1}(3d)$ (see figure 1).

data of the Oak Ridge group (Pindzola *et al* 1984) which are in excellent agreement with our measurements, except that our data do not show the small feature near 600 eV which was observed in the Oak Ridge experiments and could not be explained.

The broken curve in figure 5 represents the BEA1 result of equation (4) for a 3d-ionisation-autoionisation contribution to $\sigma_{4,6}$. The agreement of this calculation with the data suggests that the indirect process involving the 3d subshell accounts for almost all of the observed double ionisation. This conclusion has already been drawn from distorted-wave calculations by Pindzola *et al* (1984). Although the experimental cross sections show a threshold energy compatible with the minimum energy (141 eV) required to remove two electrons from Kr^{4+}, the importance of direct double ionisation is small. The BEA2 cross section from equation (5) (full curve in figure 5) is only about 5% of the experimental $\sigma_{4,6}$ at maximum.

3.2. Triple ionisation

Electron impact triple ionisation cross sections $\sigma_{q,q+3}$ for the processes

$$e + Kr^{q+} \rightarrow Kr^{(q+3)+} + 4e \qquad q = 1, 2 \tag{6}$$

were measured in the electron energy range from below threshold up to 700 eV (1000 eV for Kr^{2+} ions). The data are listed in table 2 together with their total uncertainty at the 95% confidence level for the statistical error. The measured cross sections $\sigma_{q,q+3}$ ($q = 1, 2$) are displayed in figure 6. Here, however, the error bars only indicate the statistical uncertainties.

The triple ionisation cross sections are roughly a factor of five smaller than the double ionisation data given in § 3.1. The experimental threshold energies are compatible with the minimum energy needed to remove three electrons from Kr^{+}(111 eV) and Kr^{2+}(151 eV) ions, respectively. In the energy range investigated, contributions of direct single ionisation of 3p or 3s subshells with subsequent double autoionisation are energetically allowed. For Kr^{+} ions the ionisation thresholds are 230 eV for the 3p and 309 eV for the 3s electrons; for Kr^{2+} ions the threshold energies are 242 eV for the 3p and 323 eV for the 3s electrons. Both cross sections $\sigma_{1,4}$ and $\sigma_{2,5}$ are of similar shape and magnitude, rising slowly from the respective threshold for direct triple ionisation to their maximum. Even the cross section $\sigma_{0,3}$ (Stephan *et al* 1980, Nagy *et al* 1980) fits well into this behaviour and is less than a factor of two larger than $\sigma_{1,4}$ at maximum.

In the following we discuss the results for Kr^{+} and Kr^{2+} ions in more detail.

3.2.1. Kr^{+} triple ionisation. Figure 7 shows the measured triple ionisation cross sections for Kr^{+} ions together with the total uncertainties. We are not aware of any calculation for direct triple ionisation of any ion by electron impact. Also, direct double ionisation involving one inner-shell electron with subsequent autoionisation cannot be treated with the BEA2 picture used in § 3.1. Hence, the only contributions that we can discuss quantitatively are the inner-shell multiple autoionisation processes. In the figure we show calculations for direct ionisation of 3p and 3s electrons, assuming 100% subsequent double autoionisation. The broken curve is the BEA1 result (see equation (4)) and the full curve was calculated from the Lotz semi-empirical formula (Lotz 1968). The differences in the calculated curves reflect typical uncertainties of such simple

Table 2. Electron impact triple ionisation cross sections $\sigma_{q,q+3}(q = 1, 2)$ for Kr^{q+} ions. Estimated total uncertainties are given including the statistical error at the 95% confidence level.

Electron energy (eV)	Cross section (10^{-19} cm^2)	Electron energy (eV)	Cross section (10^{-19} cm^2)
$\sigma_{1,4}$: $Kr^+ \rightarrow Kr^{4+}$			
80.0	0.09 ± 0.09	237.0	14.2 ± 1.0
90.0	0.25 ± 0.29	251.0	15.4 ± 1.0
100.0	0.15 ± 0.06	265.0	16.4 ± 1.1
110.0	0.43 ± 0.18	280.0	17.2 ± 1.1
115.0	0.50 ± 0.11	290.0	18.0 ± 1.2
125.0	1.07 ± 0.12	300.0	18.9 ± 1.2
135.0	1.57 ± 0.10	322.0	20.0 ± 1.3
145.0	2.77 ± 0.19	345.0	21.3 ± 1.4
155.0	4.79 ± 0.31	360.0	22.9 ± 1.5
165.0	6.27 ± 0.41	390.0	23.3 ± 1.5
175.0	7.43 ± 0.48	425.0	24.3 ± 1.5
185.0	8.61 ± 0.55	460.0	25.2 ± 1.6
195.0	9.66 ± 0.61	500.0	26.8 ± 1.7
206.0	10.7 ± 0.7	550.0	25.1 ± 1.6
217.0	11.9 ± 0.7	598.0	25.4 ± 1.6
230.0	13.1 ± 0.8		
$\sigma_{2,5}$: $Kr^{2+} \rightarrow Kr^{5+}$			
100.0	0.26 ± 0.48	250.0	6.29 ± 0.43
120.0	0.35 ± 0.28	270.0	8.02 ± 0.51
130.0	0.40 ± 0.41	300.0	10.1 ± 0.6
140.0	0.56 ± 0.34	320.0	10.8 ± 0.7
150.0	0.12 ± 0.18	350.0	13.1 ± 0.9
155.0	−0.02 ± 0.44	400.0	14.4 ± 0.9
160.0	0.69 ± 0.32	450.0	16.1 ± 1.0
165.0	1.02 ± 0.34	500.0	16.4 ± 1.0
170.0	1.19 ± 0.26	550.0	16.7 ± 1.1
180.0	1.66 ± 0.24	600.0	17.4 ± 1.1
190.0	2.07 ± 0.28	700.0	17.3 ± 1.1
200.0	2.65 ± 0.23	850.0	17.0 ± 1.1
210.0	3.39 ± 0.33	1000.0	16.2 ± 1.0
225.0	3.92 ± 0.29		

predictions. Anyway, it can be concluded that the inner-shell process can be responsible for much of the observed triple ionisation at energies above several hundred eV.

The 3d subshell of Kr^+ can be ionised by 105 eV electrons, i.e. the resulting 3d vacancy apparently does not provide sufficient potential energy for a double autoionisation process. However, the respective potential energies are all theoretical and calculations by Pindzola *et al* (1984) and Fricke (1985), which both include relativistic effects, differ by up to 2%. Considering uncertainties of that order and taking into account that the different levels of the 3d vacancy configuration are spread over several eV there may be a chance for some of these levels to allow for double autoionisation. In principle, a contribution from the 3d subshell could also explain the triple ionisation just above threshold.

However, a simple addition of the 3d, 3p and 3s contributions would always give rise to a distinct step in the cross section at the threshold of the 3p ionisation (230 eV)

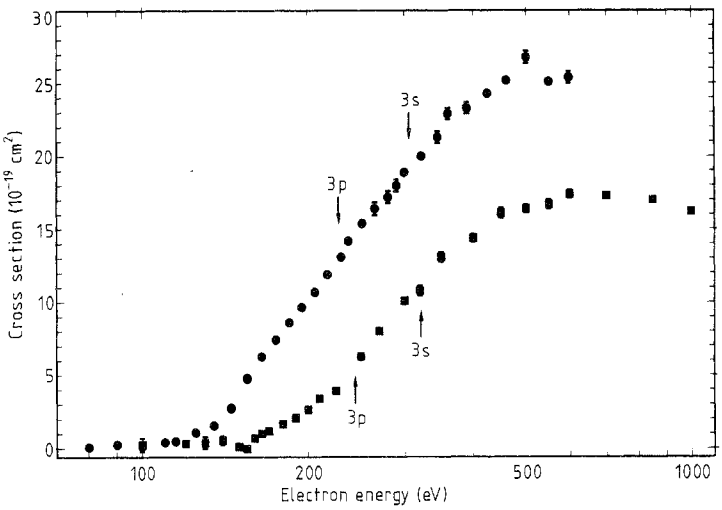

Figure 6. Present measurements of cross sections $\sigma_{q,q+3}(q = 1, 2)$ for triple ionisation of Kr^{q+} ions: ●, $\sigma_{1,4}$; ■, $\sigma_{2,5}$. Error bars show the statistical error at the 95% confidence level. Arrows mark inner-shell ionisation thresholds.

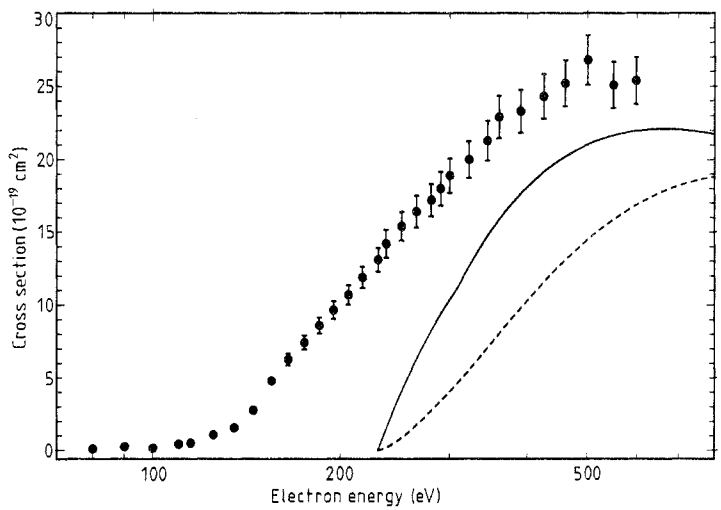

Figure 7. Present experimental results $\sigma_{1,4}$ for triple ionisation of Kr^+ ions; the error bars show the total experimental uncertainties. Also shown are the predictions of the Lotz formula (Lotz 1968, full curve) and the BEA1 (broken curve) for inner-shell single ionisation including contributions from the 3p and 3s subshells. Both curves have their onsets at the 3p-ionisation threshold.

and the experiment does not show any evidence for such a feature. In addition, there is also a possibility for 3p and 3s excitation followed by triple autoionisation which could straddle the 3p ionisation threshold and lead to a smooth total triple ionisation cross section. The probability for such a mechanism is not known.

3.2.2. Kr^{2+} triple ionisation. Figure 8 shows the measured triple ionisation cross section for Kr^{2+} ions together with the total uncertainties. The theoretical situation is the same as for Kr^{+} ions: a quantitative picture can only be given for the 3p and 3s inner-shell contributions. The chain curve represents the calculation from the Lotz formula, multiplied by a factor of 0.65 (see below). It suggests that the processes considered can account for most of the triple ionisation observed at electron energies above 250 eV. Moreover, the experimental data show an increase in slope above the 3p ionisation threshold, indicating the importance of a 3p ionisation-double autoionisation mechanism. For the range 151-242 eV we assume predominantly direct triple ionisation.

We have also tried to fit the experimental points by the sum of two contributions calculated with Lotz-type formulae in order to extract information about the branching ratio x for double autoionisation subsequent to 3p and 3s inner-shell direct single ionisation. The branching ratio is defined by $x = A_a^{(2)}/(A_r + \Sigma_i A_a^{(i)})$ with the rates $A_a^{(i)}$ for i-fold autoionisation and the total radiative rate A_r. The first of these two contributions is solely responsible for the data between 151 (threshold for direct triple ionisation) and 242 eV (3p ionisation threshold), while the sum of both contributions (the second contribution represents 3p and 3s single ionisation followed by double autoionisation)

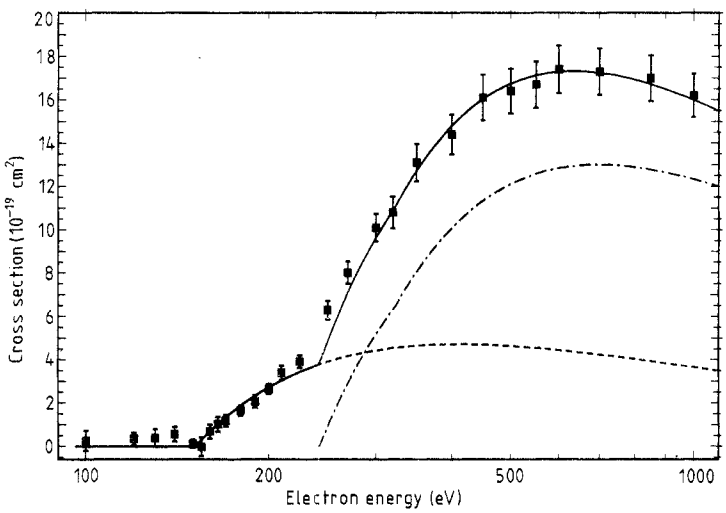

Figure 8. Present experimental results $\sigma_{2,5}$ for triple ionisation of Kr^{2+} ions; error bars show the total experimental uncertainties. The broken curve is the result of a fit through the data points between the thresholds for direct triple ionisation and for single ionisation of a 3p inner-shell electron by using a Lotz-type formula as described in the text. The chain curve represents a Lotz calculation for inner-shell single ionisation including 3p and 3s subshells scaled by a factor of 0.65. The full curve results when the broken and the chain curves are added. The chain curve represents a Lotz calculation for inner-shell single ionisation including 3p and 3s subshells scaled by a factor of 0.65 and has its onset at the 3p-ionisation threshold.

accounts for the observed cross section above 242 eV. The fit curve used is

$$\sigma = A\frac{\ln(E/P)}{EP} + x\sigma_{\mathrm{L}}(3\mathrm{p}, 3\mathrm{s}) \tag{7}$$

where $P = 151$ eV and σ_{L} is the Lotz cross section for direct 3p and 3s single ionisation. The parameter A is determined from the data in the electron energy range $151 \leqslant E \leqslant 242$ eV and amounts to 2.9×10^{-14} eV^2 cm^2. The related direct triple ionisation contribution to σ in equation (7) is represented by the broken curve in figure 8. A scaling factor $x = 0.65$ for the 3p and 3s ionisation–double autoionisation contributions (chain curve in figure 8) would fit the hypothesis underlying equation (7). The resulting total cross section σ (full curve in figure 8) gives a perfect representation of the experimental data. Apart from the fact that the data can be nicely reproduced on the basis of the hypothesis of a direct and a multi-step ionisation contribution, the above analysis does not yield information about the mechanism of direct triple ionisation which may be responsible for the cross section observed at electron energies below 242 eV.

3.3. Multiple against single ionisation

Multiple ionisation has been shown previously to occur with high probability in complex ions such as Xe^{q+} (Müller *et al* 1984). The influence of these processes on the charge state evolution, e.g. in an electron-beam ion source (EBIS) (Donets and Ovsyannikov 1981) may lead to strongly reduced containment factors $n\tau$ (n = electron density, τ = containment time) needed to produce optimum yield of ions in a given charge state (Müller 1986). The situation for Kr ions is elucidated by figures 9(a) and 9(b), which show ratios of cross sections $R_2^{(q)} = \sigma_{q,q+2}/\sigma_{q,q+1}$ and $R_3^{(q)} = \sigma_{q,q+3}/\sigma_{q,q+1}$, respectively, as a function of electron energy E. The $\sigma_{q,q+1}$ data were taken from Tinschert *et al* (1987).

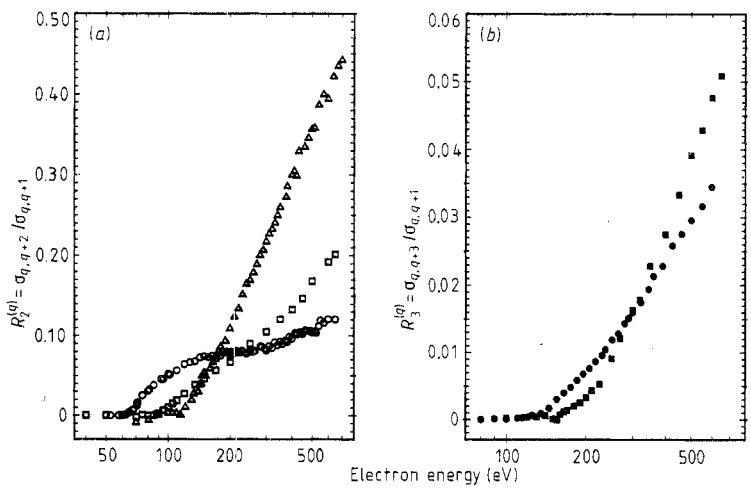

Figure 9. Ratios of multiple against single ionisation cross sections evaluated from the present measurements. The single ionisation cross sections are taken from Tinschert *et al* (1987). (a) Ratios $R_2^{(q)} = \sigma_{q,q+2}/\sigma_{q,q+1}$: ○, $\sigma_{1,3}/\sigma_{1,2}$ ($q = 1$); □, $\sigma_{2,4}/\sigma_{2,3}$ ($q = 2$); Δ, $\sigma_{3,5}/\sigma_{3,4}$ ($q = 3$). (b) Ratios $R_3^{(q)} = \sigma_{q,q+3}/\sigma_{q,q+1}$: ●, $\sigma_{1,4}/\sigma_{1,2}$ ($q = 1$); ■, $\sigma_{2,5}/\sigma_{2,3}$ ($q = 2$).

For all charge states $R_2^{(q)}$ increases with E. Above $E \simeq 200$ eV the ratios $R_2^{(3)}: R_2^{(2)}: R_2^{(1)}$ roughly behave as 10:5:3, quite independent of E. In the investigated energy range, $R_2^{(3)} = \sigma_{3,5}/\sigma_{3,4}$ nearly reaches 0.5. Since there are no data for $\sigma_{4,5}$ we do not know $R_2^{(4)} = \sigma_{4,6}/\sigma_{4,5}$. It can be expected, however, that $R_2^{(4)}$ is above 0.5 at 700 eV, since the double ionisation cross sections presented in this paper for $q = 1$-4 tend to be nearly equal at 700 eV, while the single ionisation cross sections $\sigma_{q,q+1}$ drop as 8:4:2 from $q = 1$-3 and so $\sigma_{4,5}$ is probably less than $\sigma_{3,4}$.

The ratios $R_3^{(q)}$ also increase with electron energy and above $E \simeq 300$ eV we find $R_3^{(2)} > R_3^{(1)}$. Compared with $R_2^{(q)}$, the ratios $R_3^{(q)}$are about a factor of ten smaller. It is apparent that more experiments should be done to clarify the dependences of such ratios at higher electron energies.

4. Conclusions

We have shown that electron impact double ionisation of Kr^{q+} ions ($q = 1, \ldots, 4$) is a likely process with cross sections as high as 10^{-17} cm^2. The dominating contribution to $\sigma_{q,q+2}$ for $q > 2$ is due to direct ionisation of an electron from the 3d subshell with subsequent autoionisation. For $q = 1$ there is a strong additional contribution at electron energies around 100 eV. The origin of this contribution is not clearly identified. From its shape and size, which resemble the feature observed previously in $\sigma_{1,3}$ for the ions Xe^+, I^+ (Achenbach *et al* 1983) and Cs^+ (Hertling *et al* 1982), we propose to look for influences such as term dependence in the continuum and giant resonance behaviour (Pindzola *et al* 1983, Younger 1986).

Triple ionisation is about a factor of five less likely than double ionisation for Kr^+ and Kr^{2+} ions at energies below 1 keV. Direct ionisation of an electron from the 3p or 3s subshell followed by the emission of two electrons in an autoionisation process appears to be the dominant contribution at the higher electron energies. The experimental threshold energies suggest that direct triple ionisation, i.e. a multiple-electron process, has to be considered and may be responsible for most of the triple ionisation close to the threshold energy.

A comparison of multiple to single ionisation of Kr^{q+} shows that cross section ratios $\sigma_{q,q+2}/\sigma_{q,q+1}$ and $\sigma_{q,q+3}/\sigma_{q,q+1}$ in the present range increase with the electron energy and also with the charge state of the ions once an energy of about 300 eV is reached. The ratio $\sigma_{3,5}/\sigma_{3,4}$ approaches a value as high as 0.5 at 700 eV.

In a recent investigation of single ionisation of Kr^{q+} ions (Tinschert *et al* 1987) we found conclusive evidence for the presence of metastable ions in the parent ion beams with $q = 2, 3$. For the present measurements we used the same electron-beam ion source and probably had similar fractions of metastable ions as in the previous experiments. The cross sections measured for multiple ionisation of Kr^{q+} ions ($q = 2, 3, 4$) tend to rise very slowly just above the lowest threshold and thus do not allow us to extract an accurate threshold energy which could give information about the presence of metastable ions.

So far, it is not clear what influence an initial small excitation would have on the multiple ionisation of an ion. An excitation energy of 3 or 4 eV which may influence a cross section for a process with a threshold of 37 eV (single ionisation of Kr^{2+} ions) might not have a large effect on a process with a threshold of 151 eV (triple ionisation of Kr^{2+} ions).

Acknowledgments

The authors acknowledge the help of G Hofmann and R Sauer during some of the present measurements. We are grateful to Professor Fricke of the University of Kassel and Professors Wunner and Ruder of the University of Tübingen for communicating calculated binding energies of electrons in different subshells of multiply charged krypton ions.

References

Achenbach C, Müller A, Salzborn E and Becker R 1983 *Phys. Rev. Lett.* **50** 2070-3
Donets E D and Ovsyannikov V P 1981 *Sov. Phys.-JETP* **53** 466-71
Fraga S, Karwowski J and Saxena K M S 1976 *Handbook of Atomic Data* (Amsterdam: Elsevier) pp 465-73
Fricke B 1985 Private communication
Gryzinski M 1965 *Phys. Rev.* **138** A336-58
Hertling D R, Feeney R K, Hughes D W and Sayle W E 1982 *J. Appl. Phys.* **53** 5427-34
Howald A M, Gregory D C, Phaneuf R A, Crandall D H and Pindzola M S 1986 *Phys. Rev. Lett.* **56** 1675-8
Lotz W 1968 *Z. Phys.* **216** 241-7
Müller A 1986 *Phys. Lett.* **113A** 415-9
Müller A, Achenbach C, Salzborn E and Becker R 1984 *J. Phys. B: At. Mol. Phys.* **17** 1427-44
Müller A and Frodl R 1980 *Phys. Rev. Lett.* **44** 29-32
Müller A, Huber K, Tinschert K, Becker R and Salzborn E 1985a *J. Phys. B: At. Mol. Phys.* **18** 2993-3009
Müller A, Tinschert K, Achenbach C, Becker R and Salzborn E 1985b *J. Phys. B: At. Mol. Phys.* **18** 3011-6
Müller A, Tinschert K, Achenbach C, Salzborn E and Becker R 1985c *Nucl. Instrum. Methods* B **10/11** 204-6
Müller A, Tinschert K, Achenbach C, Salzborn E, Becker R and Pindzola M S 1985d *Phys. Rev. Lett.* **54** 414-7
Nagy P, Skutlartz A and Schmidt V 1980 *J. Phys. B: At. Mol. Phys.* **13** 1249-67
Peart B and Dolder K T 1969 *J. Phys. B: At. Mol. Phys.* **2** 1169-75
Pindzola M S, Griffin D C and Bottcher C 1983 *J. Phys. B: At. Mol. Phys.* **16** L355-60
Pindzola M S, Griffin D C, Bottcher C, Crandall D H, Phaneuf R A and Gregory D C 1984 *Phys. Rev.* A **29** 1749-56
Stephan K, Helm H and Märk T D 1980 *J. Chem. Phys.* **73** 3763-78
Tinschert K, Müller A, Hofmann G, Achenbach C, Salzborn E and Becker R 1987 *J. Phys. B: At. Mol. Phys.* in press
Younger S M 1986 *Phys. Rev. Lett.* **56** 2618-20